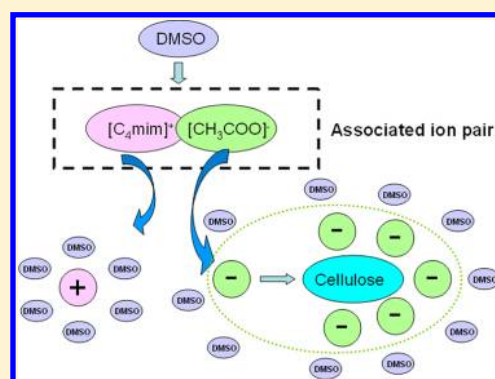


# Insight into the Cosolvent Effect of Cellulose Dissolution in Imidazolium-Based Ionic Liquid Systems

Yuling Zhao,<sup>†</sup> Xiaomin Liu,<sup>‡</sup> Jianji Wang,<sup>\*,†</sup> and Suojang Zhang<sup>\*,‡</sup><sup>†</sup>School of Chemistry and Chemical Engineering, Key Laboratory of Green Chemical Media and Reactions, Ministry of Education, Henan Normal University, Xinxiang, Henan 453007, P. R. China<sup>‡</sup>Beijing Key Laboratory of Ionic Liquids Clean Process, State Key Laboratory of Multiphase Complex Systems, Institute of Process Engineering, Chinese Academy of Sciences, Beijing 100190, P. R. China

## S Supporting Information

**ABSTRACT:** Recently, it has been reported that addition of a cosolvent significantly influences solubility of cellulose in ionic liquids (ILs), but little is known about the influence mechanism of the cosolvent on the molecular level. In this work, four kinds of typical molecular solvents (dimethyl sulfoxide (DMSO), *N,N*-dimethylformamide (DMF), CH<sub>3</sub>OH, and H<sub>2</sub>O) were used to investigate the effect of cosolvents on cellulose dissolution in [C<sub>4</sub>mim][CH<sub>3</sub>COO] by molecular dynamics simulations and quantum chemistry calculations. It was found that dissolution of cellulose in IL/cosolvent systems is mainly determined by the hydrogen bond interactions between [CH<sub>3</sub>COO]<sup>−</sup> anions and the hydroxyl protons of cellulose. The effect of cosolvents on the solubility of cellulose is indirectly achieved by influencing such hydrogen bond interactions. The strong preferential solvation of [CH<sub>3</sub>COO]<sup>−</sup> by the protic solvents (CH<sub>3</sub>OH and H<sub>2</sub>O) can compete with the cellulose–[CH<sub>3</sub>COO]<sup>−</sup> interaction in the dissolution process, resulting in decreased cellulose solubility. On the other hand, the aprotic solvents (DMSO and DMF) can partially break down the ionic association of [C<sub>4</sub>mim][CH<sub>3</sub>COO] by solvation of the cation and anion, but no preferential solvation was observed. The dissociated [CH<sub>3</sub>COO]<sup>−</sup> would readily interact with cellulose to improve the dissolution of cellulose. Furthermore, the effect of the aprotic solvent-to-IL molar ratio on the dissolution of cellulose in [C<sub>4</sub>mim][CH<sub>3</sub>COO]/DMSO systems was investigated, and a possible mechanism is proposed. These simulation results provide insight into how a cosolvent affects the dissolution of cellulose in ILs and may motivate further experimental studies in related fields.



## 1. INTRODUCTION

With fossil fuel resources decreasing and environmental pollution problems increasing, energy production from renewable biomass is a new and important undertaking. As the most abundant biorenewable resource found on the Earth, cellulose has been widely used because of its many appealing properties such as biocompatibility, biodegradability, and thermal and chemical stability.<sup>1</sup> Generally, processing cellulose into desired products first requires the dissolution of cellulose. It is known that cellulose is insoluble in water and common organic solvents, so organic solvent/water/inorganic salt mixtures<sup>2</sup> have been used to break the highly ordered crystalline structure of cellulose, which is stabilized by numerous inter- and intramolecular hydrogen bonds. However, most reported solvents have drawbacks of one kind or another, such as volatility, toxicity, high cost, difficulty in solvent recovery, high processing temperature, and process instability.<sup>3</sup> Therefore, it is imperative to develop greener solvents for cellulose dissolution under mild conditions.

Room-temperature ionic liquids (ILs) are considered to be powerful “green” solvents as they have negligible vapor pressure and high thermal stability and are nonflammable.<sup>4–6</sup> It was

reported in 2002 for the first time that cellulose can be directly dissolved in imidazolium-based ILs without any pretreatment, and the dissolved cellulose can be easily regenerated by precipitation upon addition of water or other common solvents.<sup>7</sup> Since then, many kinds of ILs have been reported to act as cellulose solvents.<sup>8–12</sup> Although significant progress has been made in this field, some problems, such as slow dissolution rate, high dissolution temperature, and high viscosity of the dissolution systems, have yet to be resolved. Thus, advances toward improved processes for the dissolution of cellulose are still necessary.

Recently, Rinaldi<sup>13</sup> found that organic solutions, which contain just a small molar fraction of IL, instantaneously dissolved large amounts of cellulose. Xu et al.<sup>14</sup> also reported several highly effective cellulose solvents consisting of 1-butyl-3-methylimidazolium acetate ([C<sub>4</sub>mim][CH<sub>3</sub>COO]) and aprotic solvents, and they suggested that the enhanced dissolution of cellulose mainly resulted from the preferential

Received: April 17, 2013

Revised: July 4, 2013

Published: July 5, 2013

solvation of cations of the IL by the cosolvents. These IL-based solvent systems circumvent the problems mentioned above in the dissolution of cellulose in neat ILs. Therefore, cellulose can be readily dissolved in the IL/cosolvent systems at ambient temperature with high solubility. Moreover, these solvent systems show many other advantages, such as nonderivatization, low viscosity, high dissolution speed, and tolerance to water. However, little is known about the molecular mechanism of these cosolvents in the dissolution of cellulose in IL-based systems.

Molecular dynamics (MD) simulations and quantum chemistry calculations are effective methods to investigate the interactions of cellulose with ILs at the molecular level. By using MD simulations, Liu et al.<sup>15</sup> investigated dissolution of (1-4) linked- $\beta$ -D-glucose oligomers with different molecular weights in  $[C_2mim][CH_3COO]$  and in other solvents, and they proposed that dissolution was promoted by the favorable interactions between the IL anions and the hydroxyl protons of glucose. Cho et al.<sup>16</sup> explained the reason why cellulose could be dissolved in  $[C_4mim]Cl$  but not in water by the idea that  $Cl^-$  anions of the IL can strongly interact with hydroxyl protons of cellulose, and the coupling of cations to side chains and linker oxygen is stronger in the peeled-off state. Balasubramanian et al.<sup>17</sup> conducted quantum chemistry calculations on a cluster of solvent molecules to solvate the cellulosic units. It was suggested that all the intramolecular hydrogen bonds were removed in the explicit  $[C_1mim][CH_3COO]$  medium because of strong H-bonding interactions between cellobiose and the IL. However, a literature survey reveals that no work investigating the cosolvent effect of cellulose dissolution in ILs at the molecular level has been reported.

In the present work, four kinds of typical cosolvents, including dimethyl sulfoxide (DMSO), *N,N*-dimethylformamide (DMF), methanol ( $CH_3OH$ ), and water ( $H_2O$ ), were chosen to study the role of cosolvents in cellulose dissolution in ILs. Among these cosolvents, DMSO and DMF are aprotic solvents, while  $CH_3OH$  and  $H_2O$  are protic solvents.  $[C_4mim][CH_3COO]$ , which shows excellent capacity for dissolving cellulose, was chosen as a model IL in the simulations. This selection makes it possible to examine the effect of cosolvent nature on the dissolution of cellulose in  $[C_4mim][CH_3COO]$ . Toward this end, MD simulations were performed on the mixtures consisting of cellulose,  $[C_4mim][CH_3COO]$ , and one of the cosolvents at 298 K. Quantum chemistry calculations were also used to reveal the interactions of cations and anions with the cosolvents. Moreover, the effect of the cosolvent-to-IL molar ratio on cellulose dissolution was investigated in  $[C_4mim][CH_3COO]$ /DMSO solvent systems, and the simulation results were compared with the experimental results. On the basis of these investigations, a possible mechanism for the dissolution of cellulose in IL/cosolvent systems was proposed.

## 2. COMPUTATIONAL DETAILS

**2.1. Molecular Dynamics Simulations. Force Field Parameters.** All-atom force fields were used in our simulations. For cellulose with a degree of polymerization (DP) of 10, the GLYCAM force field<sup>18</sup> was used, and the SPC model<sup>19</sup> was employed for water molecules. For DMSO,<sup>20</sup> DMF,<sup>21</sup>  $CH_3OH$ ,<sup>20</sup> and  $[C_4mim][CH_3COO]$ <sup>22</sup> (see Figure 1 for their chemical structures), the reported parameters of the AMBER force field were always used. Optimization of the isolated ion structures was performed by using Gaussian 09 (version

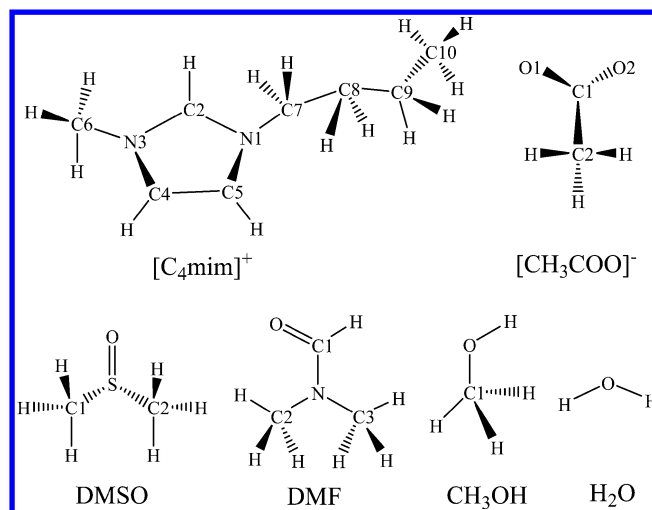


**Figure 1.** Chemical structures for  $[C_4mim][CH_3COO]$  and different cosolvents.

B.01)<sup>23</sup> at the B3LYP/6-31+G\* level of theory. Atom charges were obtained by fitting the electrostatic potentials calculated at the B3LYP/6-311++G\* level of theory, and a one-conformation, two-step restraint electrostatic potential method was used for this purpose.<sup>24</sup>

**Simulation Details.** All simulations were performed with the MDynaMix 5.2 package.<sup>25</sup> The double-time-step algorithm<sup>26</sup> was adopted with long and short time steps of 2 and 0.5 fs, respectively. The Ewald summation method<sup>27</sup> was used to treat the long-range electrostatic interaction, in which the long-range parts were cut off at 15 Å. The simulations were first performed using mixtures of  $[C_4mim][CH_3COO]$  with different cosolvents at the same cosolvent-to-IL molar ratio. Then additional simulations were carried out on the mixtures of cellulose with  $[C_4mim][CH_3COO]$ /DMSO solvent as a function of the molar ratio. All simulations were carried out at 298 K. The initial configuration was prepared by PACKMOL<sup>28</sup> in a rectangle box, typically larger than the “real” size to make the packing easier, and the cellulose chain was aligned along the *x*-direction of the box. Every simulation system consisted of one cellulose chain with DP = 10,  $[C_4mim][CH_3COO]$ , and different cosolvents. The number of solvent molecules and cosolvent-to-IL molar ratio for each IL/cosolvent system are given in Supporting Information, Table S1.

A starting simulation was carried out at 700 K in the NVE ensemble. After relaxation for a few MD steps to reduce the possible overlap with the initial configuration, the Nose–Hoover NPT ensemble simulation<sup>29</sup> was performed. After the temperature had decreased from 700 K to the sampling temperature of 298 K, a series of NPT simulations were carried out under standard atmospheric conditions. At the sampling temperature point, the system was equilibrated for at least 5 ns. Then the production phase lasted for 4 ns. The conformations in trajectories were dumped for further analysis with an interval of 20 fs. After the simulation, the interaction energies for these systems were calculated. In the mixture system of cellulose, IL, and cosolvent, all the interaction energies between two molecular types are given per mole of the substance that is present in a smaller amount. Therefore, the interaction energy of IL or cosolvent with cellulose is per mole of cellulose, whereas the interaction energy of IL with cosolvent is per mole of IL.

**2.2. Quantum Chemistry Calculations.** The pairs  $[\text{CH}_3\text{COO}]^-$ -DMSO,  $[\text{CH}_3\text{COO}]^-$ -DMF,  $[\text{CH}_3\text{COO}]^-$ - $\text{CH}_3\text{OH}$ ,  $[\text{CH}_3\text{COO}]^-$ - $\text{H}_2\text{O}$ ,  $[\text{C}_4\text{mim}]^+$ -DMSO, and  $[\text{C}_4\text{mim}]^+$ -DMF and the isolated ions were optimized by Gaussian 09.<sup>23</sup> The structural optimizations were carried out at the popular B3LYP/6-311++G(d,p) theoretical level. All the optimized geometries were recognized as local minima without any negative vibrational frequency. The initial configurations of the ion-molecule pairs were mainly based on the charge distribution and electrostatic potential on the isolated cation and anion. Thus, the favored position of the cosolvents was distributed around the C2, C4, and C5 sites of the  $[\text{C}_4\text{mim}]^+$  cation and the O1 and O2 sites of the  $[\text{CH}_3\text{COO}]^-$  anion (see the atom numbering in Figure 1). The interaction energies were obtained at the B3LYP/6-311++G(d,p) level of theory with basis set superposition error (BSSE) correction, and natural population analyses (NPA) of the conformers were also carried out using Gaussian 09.<sup>23</sup>

### 3. RESULTS AND DISCUSSION

**3.1. Cosolvent Effect of Cellulose Dissolution in the  $[\text{C}_4\text{mim}][\text{CH}_3\text{COO}]$  Solvent Systems.** To understand the action mechanism of a cosolvent in cellulose dissolution, a series of MD simulations were performed on the mixtures of  $[\text{C}_4\text{mim}][\text{CH}_3\text{COO}]$  and cellulose with and without cosolvent at 298 K. Because the maximum cellulose solubility was experimentally found to be  $R_{\text{DMSO}} = 2.54$  (where  $R_{\text{DMSO}}$  is the molar ratio of DMSO to  $[\text{C}_4\text{mim}][\text{CH}_3\text{COO}]$ ),<sup>3</sup> this molar ratio was used in the simulations of the  $[\text{C}_4\text{mim}][\text{CH}_3\text{COO}]/\text{cellulose}/\text{DMSO}$  mixtures. In order to facilitate the comparison of simulation data, the molar ratio of 2.54 was also used for the simulations involving other cosolvents. After such simulations, interaction energies of the cation, anion, and cosolvents with cellulose in the  $[\text{C}_4\text{mim}][\text{CH}_3\text{COO}]/\text{cellulose}/\text{DMSO}$  systems were calculated by the sum of electrostatic and van der Waals energies. It can be seen from Figure 2 that the interaction

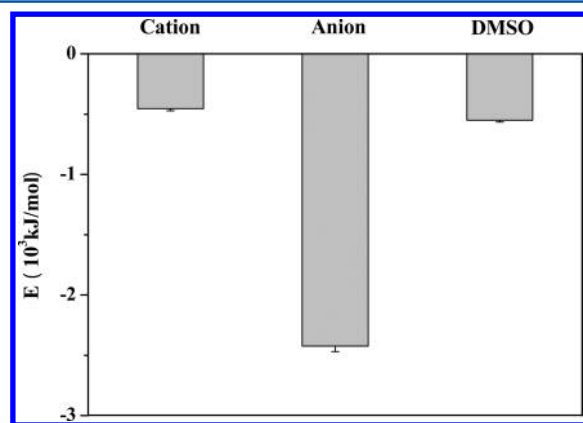


**Figure 2.** Interaction energies of cellulose with cations, anions, and cosolvent in the  $[\text{C}_4\text{mim}][\text{CH}_3\text{COO}]/\text{cellulose}/\text{DMSO}$  system obtained from MD simulations.

energy of the anion with cellulose is significantly higher than that of the cation and DMSO with cellulose. This suggests that, similar to the dissolution in neat ILs, the dissolution of cellulose in IL/cosolvent systems is still mainly determined by the hydrogen bond interaction between  $[\text{CH}_3\text{COO}]^-$  and the hydroxyl protons of cellulose. The cosolvent has only an indirect effect on the solubility of cellulose by influencing the

interaction between  $[\text{CH}_3\text{COO}]^-$  and cellulose. Thus, the interaction energies of  $[\text{CH}_3\text{COO}]^-$  with cellulose in  $[\text{C}_4\text{mim}][\text{CH}_3\text{COO}]/\text{cellulose}/\text{cosolvent}$  systems were calculated and compared with that in the  $[\text{C}_4\text{mim}][\text{CH}_3\text{COO}]/\text{cellulose}$  system to understand the effect of cosolvents on cellulose solubility (Table 1). It can be seen from Table 1 that the

**Table 1. Interaction Energies between Anions and Cellulose Obtained from MD Simulations in Different Systems**

system	$E_{\text{ele}}^a$ (kJ/mol)	$E_{\text{vdw}}^b$ (kJ/mol)	$E_{\text{inter}}^c$ (kJ/mol)
$[\text{C}_4\text{mim}][\text{CH}_3\text{COO}]/\text{cellulose}/\text{DMSO}$	-2599.8	176.4	$-2423.5 \pm 45.1$
$[\text{C}_4\text{mim}][\text{CH}_3\text{COO}]/\text{cellulose}/\text{DMF}$	-2321.6	139.9	$-2181.7 \pm 50.5$
$[\text{C}_4\text{mim}][\text{CH}_3\text{COO}]/\text{cellulose}$	-1930.9	19.7	$-1911.2 \pm 39.0$
$[\text{C}_4\text{mim}][\text{CH}_3\text{COO}]/\text{cellulose}/\text{CH}_3\text{OH}$	-1981.4	109.3	$-1872.1 \pm 40.4$
$[\text{C}_4\text{mim}][\text{CH}_3\text{COO}]/\text{cellulose}/\text{H}_2\text{O}$	-1750.2	-29.2	$-1779.4 \pm 42.1$

<sup>a</sup> $E_{\text{ele}}$ , electrostatic interaction energy. <sup>b</sup> $E_{\text{vdw}}$ , van der Waals interaction energy. <sup>c</sup> $E_{\text{inter}}$ , the sum of  $E_{\text{ele}}$  and  $E_{\text{vdw}}$ .

electrostatic interaction is much stronger than the van der Waals interaction, indicating that the electrostatic portion dominates the interaction between anions and cellulose. It should be pointed out that in the calculation of the electrostatic energies, the software used by us includes not only the electrostatic interaction but also the hydrogen bond interaction. Thus, electrostatic and hydrogen bond interactions are the main interactions between  $[\text{CH}_3\text{COO}]^-$  and cellulose. When a cosolvent is added to the IL, the energy change in the electrostatic portion is larger than that in the van der Waals portion. This suggests that addition of a cosolvent has a significant influence on the electrostatic and hydrogen bond interactions between the anion and cellulose. We also found that the anion-cellulose interaction increased as DMSO or DMF was added to the IL but decreased on addition of  $\text{CH}_3\text{OH}$  or  $\text{H}_2\text{O}$  to the system. Therefore, the addition of an aprotic solvent to the IL results in increased cellulose solubility, whereas the addition of a protic solvent leads to decreased cellulose solubility. This conclusion is in good agreement with the results reported in the literature;<sup>1,4</sup> thus, experimental results have been predicted qualitatively by our MD simulations.

It was reported that strong ionic association was present in neat ILs by electrostatic and hydrogen bonding interactions.<sup>30</sup> Thus, their dissociation degree would be crucial to the dissolution of cellulose in ILs. To examine the effect of a cosolvent on the dissociation of ILs, the interaction energies of the anions with cations in  $[\text{C}_4\text{mim}][\text{CH}_3\text{COO}]/\text{cellulose}$  and  $[\text{C}_4\text{mim}][\text{CH}_3\text{COO}]/\text{cellulose}/\text{cosolvent}$  systems were calculated, and the results are shown in Figure 3. It is clearly indicated that the interaction energy between cations and anions in IL/cellulose system is remarkably higher than those in IL/cellulose/cosolvent systems. This suggests that a fraction of the anions were associated with cations in the IL/cellulose system. When a cosolvent was added to the IL, the association between cation and anion was partially broken down to produce more free anions and cations. The degree of cosolvent effect decreases in the order  $\text{DMSO} > \text{DMF} > \text{CH}_3\text{OH} > \text{H}_2\text{O}$ . It seems likely that the decrease in cation-anion interactions is caused by the size of the cosolvent as the molar volumes of



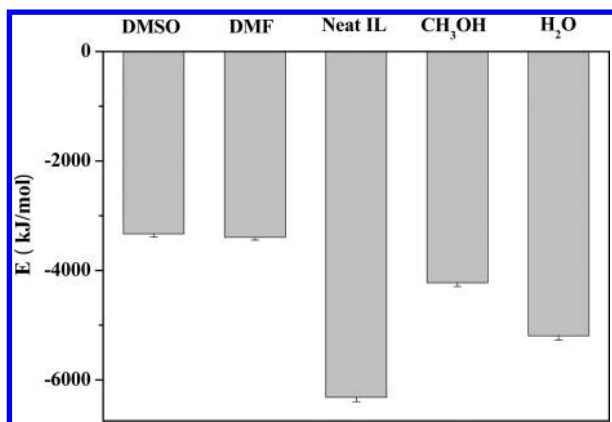


**Figure 3.** Interaction energies between anions and cations in neat  $[\text{C}_4\text{mim}][\text{CH}_3\text{COO}]$  and  $[\text{C}_4\text{mim}][\text{CH}_3\text{COO}]/\text{cellulose}/\text{cosolvent}$  mixtures obtained from MD simulations.

DMSO and DMF are larger than those of  $\text{CH}_3\text{OH}$  and  $\text{H}_2\text{O}$ . To confirm this speculation, another cosolvent, propanol ( $\text{CH}_3\text{CH}_2\text{CH}_2\text{OH}$ ), which has a molar volume similar to that of DMSO ( $75.2 \text{ cm}^3 \text{ mol}^{-1}$  vs  $71.3 \text{ cm}^3 \text{ mol}^{-1}$  at 298 K, respectively), was chosen and the interaction energies between cations and anions of the IL in both systems were calculated and compared. It was shown that the effects of DMSO and  $\text{CH}_3\text{CH}_2\text{CH}_2\text{OH}$  on the cation–anion interactions are roughly the same. This suggests that the addition of a larger cosolvent is favorable to the ionic dissociation of ILs. Because more free anions were produced in the presence of cosolvents, it is difficult to understand why the interaction between  $[\text{CH}_3\text{COO}]^-$  and cellulose was reduced upon addition of protic solvents in the IL. At this stage, it is reasonable to speculate that in the presence of an aprotic solvent more dissociated anions take part in the interaction with cellulose, but the dissociated anions resulting from the addition of protic solvents may have been solvated strongly by the cosolvents.

In order to confirm this speculation, spatial distribution functions (SDFs) of the cosolvents around  $[\text{CH}_3\text{COO}]^-$  were calculated, and the results are shown in Figure 4. The coordinate lengths in the  $x$ -,  $y$ -, and  $z$ -directions were chosen to be 20 Å in the calculations, and the green contour surface was drawn at 3 times the average density. As depicted in Figure 4, DMSO and DMF molecules were mainly distributed in a circle along the C1–C2 axis of  $[\text{CH}_3\text{COO}]^-$ , while  $\text{CH}_3\text{OH}$  and  $\text{H}_2\text{O}$  were mainly distributed around the O1 and O2 sites of  $[\text{CH}_3\text{COO}]^-$ . As the O1 and O2 atoms of  $[\text{CH}_3\text{COO}]^-$  can form strong hydrogen bonds with hydroxyl protons of cellulose, the distribution of  $\text{CH}_3\text{OH}$  and  $\text{H}_2\text{O}$  around the O1 and O2 sites of  $[\text{CH}_3\text{COO}]^-$  would hinder the interaction between anions and cellulose. This suggests that the interaction of protic solvents with  $[\text{CH}_3\text{COO}]^-$  can compete with the interaction of cellulose with  $[\text{CH}_3\text{COO}]^-$ , resulting in the decreased interaction between cellulose and  $[\text{CH}_3\text{COO}]^-$ . However, aprotic solvents like DMSO and DMF do not have such a competition for  $[\text{CH}_3\text{COO}]^-$ . In addition, the interaction energies between the anion and the cosolvents were also calculated for these systems (Figure 5). It can be seen that in the IL/cellulose/cosolvent systems the interactions between anions and protic solvents are significantly stronger than those between anions and aprotic solvents. This indicates that the protic solvents favorably interact with anions and then weaken the interaction between anions and cellulose, leading to the

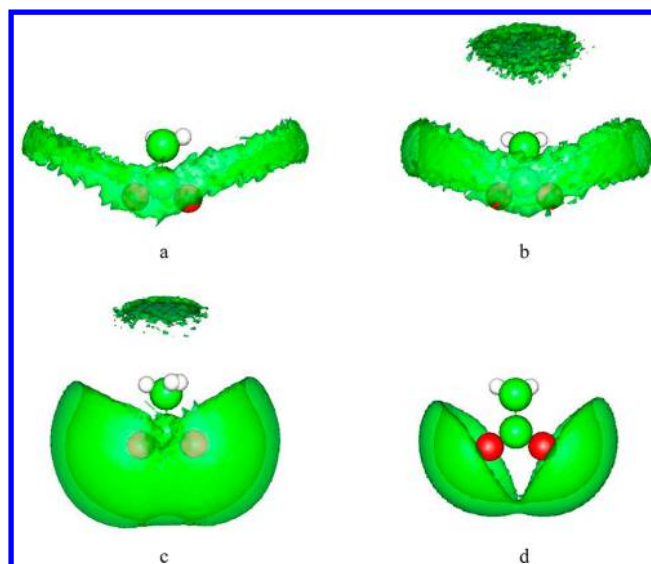


**Figure 4.** Spatial distribution functions of the central atom of different cosolvents around  $[\text{CH}_3\text{COO}]^-$ : a, the S atom of DMSO; b, the N atom of DMF; c, the C atom of  $\text{CH}_3\text{OH}$ ; and d, the O atom of  $\text{H}_2\text{O}$ .

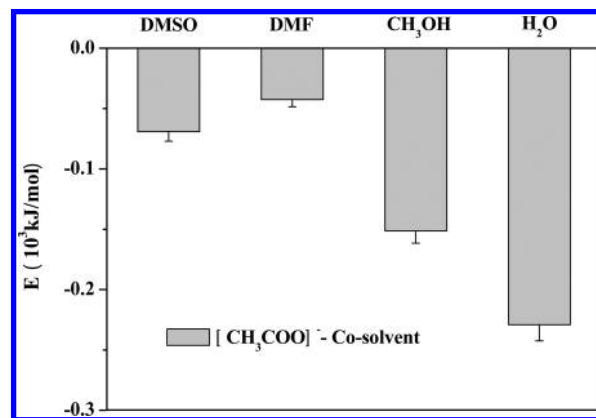


**Figure 5.** Interaction energies of  $[\text{CH}_3\text{COO}]^-$  with cosolvents in the systems obtained by MD simulations at 298 K.

decrease in cellulose solubility. On the contrary, the interactions between the aprotic solvents and the dissociated  $[\text{CH}_3\text{COO}]^-$  anions are weak; thus, these anions would readily interact with cellulose, leading to the increase in cellulose solubility.

**3.2. The Ionic Solvation of  $[\text{C}_4\text{mim}][\text{CH}_3\text{COO}]$  by Different Cosolvents from Quantum Chemistry Calculations.** From the above discussion, it is clear that the solvation mechanism of  $[\text{C}_4\text{mim}][\text{CH}_3\text{COO}]$  in aprotic solvents is different from that in protic solvents. In order to analyze the nature of ionic solvation of the IL by the cosolvents, ion–molecule pairs of  $[\text{CH}_3\text{COO}]^-$  and  $[\text{C}_4\text{mim}]^+$  with different cosolvents were optimized, and their interaction energies were calculated by quantum chemistry calculations at the B3LYP/6-311++G(d,p) level of theory.

First, we focus our attention on the optimized structures of  $[\text{CH}_3\text{COO}]^-$  and  $[\text{C}_4\text{mim}]^+$  with different cosolvents. The lowest-energy conformers for  $[\text{CH}_3\text{COO}]^-$ –cosolvent pairs are shown in Figure 6. It is clear that the O of  $[\text{CH}_3\text{COO}]^-$  could form hydrogen bonds with methyl H in DMSO and DMF molecules. The length of the C–H...O hydrogen bond is  $\sim 2.07$ – $2.18$  Å, which is generally regarded as a weak hydrogen

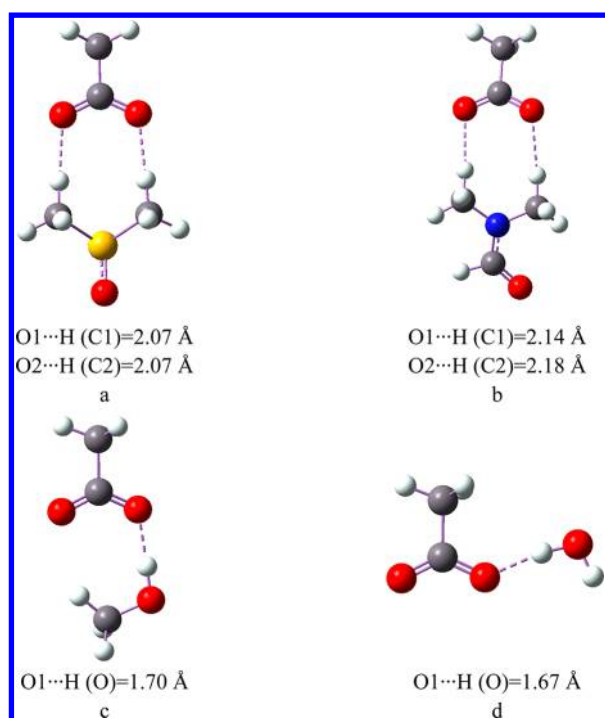


**Figure 6.** Optimized geometries for ion–molecule pairs of  $[\text{CH}_3\text{COO}]^-$  with different cosolvent molecules: a, DMSO; b, DMF; c,  $\text{CH}_3\text{OH}$ ; and d,  $\text{H}_2\text{O}$ . The dashed lines indicate hydrogen bonds in these pairs. C (gray), H (white), O (red), S (yellow), and N (blue) are shown in different colors for clarity.

bond. However, for  $\text{CH}_3\text{OH}$  and  $\text{H}_2\text{O}$ , the  $\text{O}-\text{H}\cdots\text{O}$  hydrogen bond was formed by a hydroxyl proton of the cosolvents with  $[\text{CH}_3\text{COO}]^-$ . The length of the  $\text{O}-\text{H}\cdots\text{O}$  hydrogen bond is  $\sim 1.67$ – $1.70$  Å, which is considered a strong hydrogen bond. The hydrogen bond formation comes with charge transfer; thus, the natural population analysis (NPA) charges of the isolated molecule and the ion–molecule pairs were calculated for these conformers. The total charge for the cosolvent molecule and  $[\text{CH}_3\text{COO}]^-$ –cosolvent pairs is shown in Table 2. It can be seen that a small charge transfer was observed for

**Table 2.** NPA Charge Change of Different Cosolvents from Isolated Molecule to  $[\text{CH}_3\text{COO}]^-$ –Cosolvent Pairs

cosolvent	isolated molecule	$[\text{CH}_3\text{COO}]^-$ –cosolvent pair
DMSO	0.0	−0.0588
DMF	0.0	−0.0427
$\text{CH}_3\text{OH}$	0.0	−0.0690
$\text{H}_2\text{O}$	0.0	−0.0600

the anion–cosolvent pairs. Comparison of the change in the total charge of different cosolvents reveals that the charge transfer decreases in the order  $\text{CH}_3\text{OH} > \text{H}_2\text{O} > \text{DMSO} > \text{DMF}$ . This suggests that the charge transfer for the  $\text{C}-\text{H}\cdots\text{O}$  hydrogen bond is smaller than that for the  $\text{O}-\text{H}\cdots\text{O}$  hydrogen bond, and the result provides further evidence for the fact that the  $\text{O}-\text{H}\cdots\text{O}$  hydrogen bond is stronger than the  $\text{C}-\text{H}\cdots\text{O}$  hydrogen bond. In addition, the optimized geometries for the ion–molecule pairs of  $[\text{C}_4\text{mim}]^+$  with different cosolvents are shown in Figure 7. It was found that the hydrogen at C2, C4, and C5 sites of  $[\text{C}_4\text{mim}]^+$  could form hydrogen bonds with the O of DMSO, DMF,  $\text{CH}_3\text{OH}$ , and  $\text{H}_2\text{O}$  and that the hydrogen bonds are of the weak  $\text{C}-\text{H}\cdots\text{O}$  type.

Next, we discuss the interaction energies of these ion–molecule pairs (Table 3), building toward a better understanding of the solvation of  $[\text{C}_4\text{mim}][\text{CH}_3\text{COO}]$  by different cosolvents. It is evident from the comparison of the interaction energies of the protic solvents with  $[\text{C}_4\text{mim}]^+$  and  $[\text{CH}_3\text{COO}]^-$  that the interaction between a protic solvent and  $[\text{CH}_3\text{COO}]^-$  is much stronger than that between a protic solvent and  $[\text{C}_4\text{mim}]^+$ . Therefore, it is reasonable to state that the  $[\text{CH}_3\text{COO}]^-$  anion is strongly preferentially solvated by the protic solvents. However, the aprotic solvent– $[\text{CH}_3\text{COO}]^-$  interaction did not differ significantly from aprotic solvent– $[\text{C}_4\text{mim}]^+$  interaction. Thus, preferential ionic solvation of  $[\text{C}_4\text{mim}][\text{CH}_3\text{COO}]$  by the aprotic solvents was not observed. To further confirm this observation, binary systems consisting of  $[\text{C}_4\text{mim}][\text{CH}_3\text{COO}]$  and different cosolvents were investigated by MD simulations and the interaction energies of cations and anions with different cosolvents were calculated (see Table S2 in Supporting Information). It was found that the  $[\text{CH}_3\text{COO}]^-$  anion is indeed preferentially solvated by the protic solvents, but  $[\text{C}_4\text{mim}]^+$  and  $[\text{CH}_3\text{COO}]^-$  are almost equally solvated by the aprotic solvents.

**3.3. Effect of the Cosolvent-to-IL Molar Ratio on Cellulose Dissolution and the Possible Dissolution Mechanism.** DMSO was chosen as an example to study the influence of the cosolvent-to- $[\text{C}_4\text{mim}][\text{CH}_3\text{COO}]$  molar ratio on cellulose solubility. For this purpose, a series of MD simulations were performed and the interaction energies between the anion of the IL and cellulose were calculated at different molar ratios at 298 K. Figure 8 shows the interaction energies of the anion with cellulose as a function of the DMSO-to-IL molar ratio. It is shown that the interaction energy first increases and then decreases with the increase in the molar ratio; the strongest interaction appears at  $R_{\text{DMSO}} = 2.54$ . The calculated interaction energies between anions and cellulose were also compared roughly with the reported experimental solubility data. It was found that the trend of the interaction energy is in agreement with the molar ratio dependence of experimental solubility reported previously<sup>14</sup> (Figure 8). As the strength of the interaction between the IL anion and cellulose increases, the solubility of cellulose in the IL/cosolvent systems also increases. Generally, the experimental solubility is easily influenced by many factors such as the source of the cellulose, the degree of polymerization of cellulose, the purity of the ILs, the temperature of dissolution, and the method of heating used in the experiments. The simulation result is influenced by the number of molecules and the degree of polymerization of cellulose. Despite these factors, the trend of our simulation results is still in good agreement with that of the experimental solubility. This indicates that the model adopted in our simulations can correctly describe the main intermolecular interactions in the mixtures of cellulose, IL, and cosolvent. Therefore, the simulated interaction energies are very useful in choosing a cosolvent to improve the dissolving capability of ILs.

Encouraged by the above results, we suggested a possible mechanism for the dissolution of cellulose in  $[\text{C}_4\text{mim}][\text{CH}_3\text{COO}]/\text{DMSO}$  systems that is described below. As we know, there are a lot of associated ion pairs in neat ILs.<sup>30</sup> When the DMSO-to-IL molar ratio is below the molar ratio corresponding to the strongest interaction (called the best molar ratio),  $[\text{C}_4\text{mim}]^+$  and  $[\text{CH}_3\text{COO}]^-$  are solvated by DMSO to partially break the ionic association in the IL. The dissociated  $[\text{CH}_3\text{COO}]^-$  would interact with cellulose, leading to the increase in cellulose solubility. At the best molar ratio,

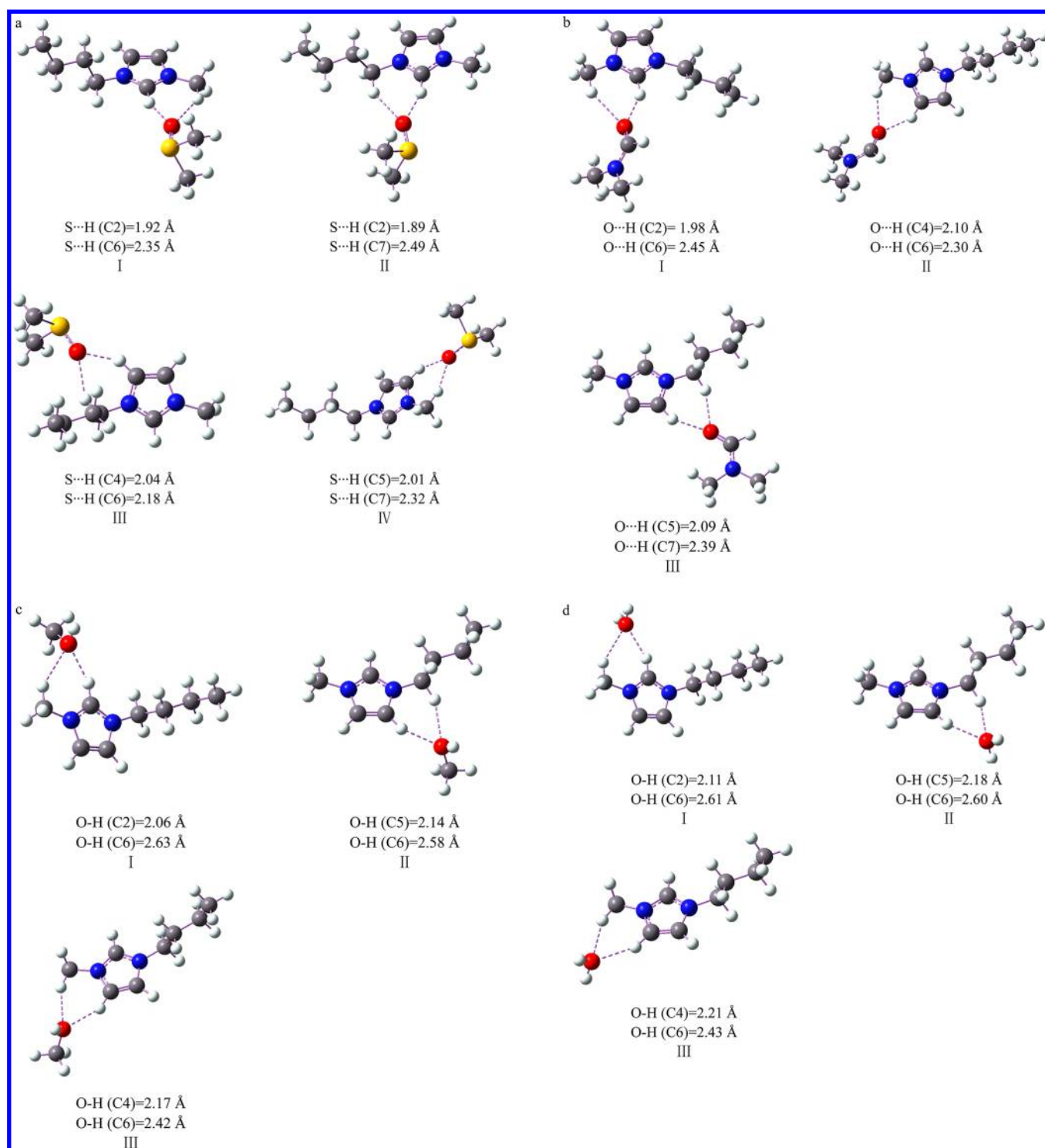


**Figure 7.** Optimized geometries for ion–molecule pairs of  $[\text{C}_4\text{mim}]^+$  with different cosolvent molecules: a, DMSO; b, DMF; c,  $\text{CH}_3\text{OH}$ ; and d,  $\text{H}_2\text{O}$ . The dashed lines indicate the hydrogen bonds in these pairs. C (gray), H (white), O (red), S (yellow), and N (blue) are shown in different colors for clarity.

ionic solvation of the IL reaches its equilibrium, and the largest number of dissociated  $[\text{CH}_3\text{COO}]^-$  would interact with cellulose. On the other hand, when the molar ratio is greater than the best molar ratio, concentrations of  $[\text{C}_4\text{mim}]^+$  and  $[\text{CH}_3\text{COO}]^-$  are gradually diluted by DMSO. This results in a decrease in the interaction between  $[\text{CH}_3\text{COO}]^-$  and cellulose and thus the decreased solubility of cellulose.

#### 4. CONCLUSION

In the present work, all-atom MD simulations and quantum chemistry calculations have been used to understand the effect of cosolvents on cellulose dissolution in  $[\text{C}_4\text{mim}][\text{CH}_3\text{COO}]$ . It is found that protic cosolvents, such as  $\text{CH}_3\text{OH}$  and  $\text{H}_2\text{O}$ , form strong O–H $\cdots$ O hydrogen bonds with  $[\text{CH}_3\text{COO}]^-$  and weak C–H $\cdots$ O hydrogen bonds with  $[\text{C}_4\text{mim}]^+$ , indicating preferential solvation of anions of the IL by the protic



**Table 3. Interaction Energies of  $[\text{CH}_3\text{COO}]^-$  and  $[\text{C}_4\text{mim}]^+$  with Different Cosolvents Obtained from Quantum Chemistry Calculations**

cosolvent	$[\text{CH}_3\text{COO}]^-$ (kJ/mol)	$[\text{C}_4\text{mim}]^+$ (kJ/mol)			
	$E_{\text{inter}}$	$E_{\text{inter}}(\text{I})$	$E_{\text{inter}}(\text{II})$	$E_{\text{inter}}(\text{III})$	$E_{\text{inter}}(\text{IV})$
DMSO	−81.9	−78.3	−75.9	−65.5	−67.9
DMF	−61.7	−69.0	−59.5	−56.7	−
$\text{CH}_3\text{OH}$	−74.5	−43.1	−34.9	−36.4	−
$\text{H}_2\text{O}$	−82.6	−44.5	−37.1	−38.4	−

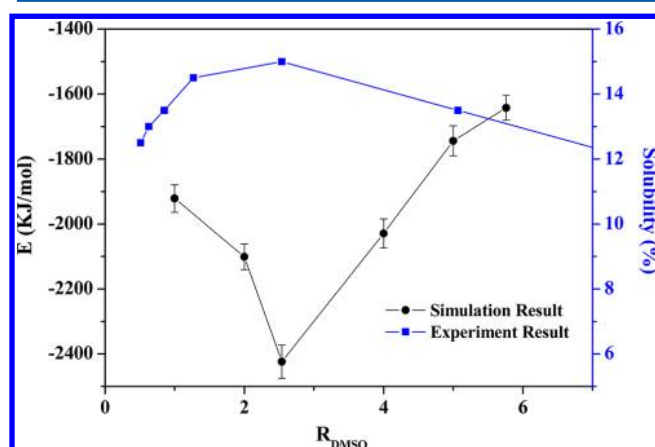


**Figure 8.** Simulated interaction energies between  $[\text{CH}_3\text{COO}]^-$  and cellulose in the IL/cellulose/DMSO systems and experimental solubility of cellulose in IL/DMSO solvents as a function of DMSO-to-IL molar ratio at 298 K.

cosolvents. However, aprotic solvents like DMSO and DMF form weak  $\text{C}-\text{H}\cdots\text{O}$  hydrogen bonds with  $[\text{C}_4\text{mim}]^+$  and  $[\text{CH}_3\text{COO}]^-$ . The strong preferential solvation of anions of the IL results in the reduced interaction between anions and cellulose and thus decreased solubility of cellulose. The solvation of  $[\text{C}_4\text{mim}]^+$  and  $[\text{CH}_3\text{COO}]^-$  by the aprotic solvents makes it possible to produce more “free”  $[\text{CH}_3\text{COO}]^-$  anions from anion–cation pairs, which would readily interact with cellulose, leading to the increase in cellulose solubility. In addition, the molar ratio (aprotic solvent to the IL) dependence of cellulose solubility is correctly predicted by our simulations. It is suggested that the trend of cellulose solubility with the molar ratio is determined by the concentration of anions of the IL.

The above findings would be great of importance for the understanding of the dissolution mechanism of cellulose in IL/cosolvent systems and for the rational design of novel highly efficient cellulose solvents. On the basis of these findings, an aprotic solvent which can increase anion concentration through its solvation is the correct choice for the cosolvent in the dissolution of cellulose in IL/cosolvent systems.

## ■ ASSOCIATED CONTENT

### ● Supporting Information

Further details including the number of solvent molecules, cosolvent-to-IL molar ratio for  $[\text{C}_4\text{mim}][\text{CH}_3\text{COO}]$ /cellulose/cosolvent systems, and the interaction energies of  $[\text{C}_4\text{mim}]^+$  and  $[\text{CH}_3\text{COO}]^-$  with the cosolvents in different  $[\text{C}_4\text{mim}][\text{CH}_3\text{COO}]$ /cosolvent systems obtained from molecular dynamics simulations. This material is available free of charge via the Internet at <http://pubs.acs.org>.

## ■ AUTHOR INFORMATION

### Corresponding Author

\*J.W.: phone, +86-373-3325805; e-mail, [jwang@henannu.edu.cn](mailto:jwang@henannu.edu.cn). S.Z.: phone, +86-10-82627080; e-mail, [sjzhang@home.ipe.ac.cn](mailto:sjzhang@home.ipe.ac.cn).

### Notes

The authors declare no competing financial interest.

## ■ ACKNOWLEDGMENTS

This work was supported by the National Basic Research Program of China (2009CB219902) and the National Natural Science Foundation of China (Grants 21133009, 21073194, and 21106146).

## ■ REFERENCES

- (1) Wang, H.; Gurau, G.; Rogers, R. D. Ionic Liquid Processing of Cellulose. *Chem. Soc. Rev.* **2012**, *41*, 1519–1537.
- (2) Abe, M.; Fukaya, Y.; Ohno, H. Extraction of Polysaccharides from Bran with Phosphonate or Phosphinate-Derived Ionic Liquids under Short Mixing Time and Low Temperature. *Green Chem.* **2010**, *12*, 1274–1280.
- (3) Xu, A. R.; Wang, J. J.; Wang, H. Y. Effects of Anionic Structure and Lithium Salts Addition on the Dissolution of Cellulose in 1-Butyl-3-Methylimidazolium-Based Ionic Liquid Solvent Systems. *Green Chem.* **2010**, *12*, 268–275.
- (4) Pinkert, A.; Marsh, K. N.; Pang, S. S.; Staiger, M. P. Ionic Liquids and Their Interaction with Cellulose. *Chem. Rev.* **2009**, *109*, 6712–6728.
- (5) *Ionic Liquids*; Zhang, S., Lu, X., et al., Eds.; Elsevier Press: Amsterdam, 2009.
- (6) Robin, D.; Zhang, S.; Wang, J. Preface: An International Look at Ionic Liquids. *Sci. China: Chem.* **2012**, *55*, 1475–1477.
- (7) Swatloski, R. P.; Spear, S. K.; Holbrey, J. D.; Rogers, R. D. Dissolution of Cellulose with Ionic Liquids. *J. Am. Chem. Soc.* **2002**, *124*, 4974–4975.
- (8) Liu, Z.; Wang, H.; Li, Z.; Lu, X.; Zhang, X.; Zhang, S.; Zhou, K. Characterization of the Regenerated Cellulose Films in Ionic Liquids and Rheological Properties of the Solutions. *Mater. Chem. Phys.* **2011**, *128*, 220–227.
- (9) Liu, Z.; Wang, H.; Li, Z.; Lu, X.; Zhang, X.; Zhang, S.; Zhou, K. Rheological Properties of Cotton Pulp Cellulose Dissolved in 1-Butyl-3-Methylimidazolium Chloride Solutions. *Polym. Eng. Sci.* **2011**, *51*, 2381–2386.
- (10) Shi, C.; Zhao, Y.; Xin, J.; Wang, J.; Lu, X.; Zhang, X.; Zhang, S. Effects of Cations and Anions of Ionic Liquids on the Production of 5-Hydroxymethylfurfural from Fructose. *Chem. Commun. (Cambridge, U.K.)* **2012**, *48*, 4103–4105.
- (11) Zhao, Y.; Liu, X.; Wang, J.; Zhang, S. Effects of Cationic Structure on Cellulose Dissolution in Ionic Liquids: A Molecular Dynamics Study. *ChemPhysChem* **2012**, *13*, 3126–3133.
- (12) Zhao, Y.; Liu, X.; Wang, J.; Zhang, S. Effects of Anionic Structure on the Dissolution of Cellulose in Ionic Liquids Revealed by Molecular Simulation. *Carbohydr. Polym.* **2013**, *94*, 723–730.
- (13) Rinaldi, R. Instantaneous Dissolution of Cellulose in Organic Electrolyte Solutions. *Chem. Commun. (Cambridge, U.K.)* **2011**, *47*, 511–513.
- (14) Xu, A.; Zhang, Y.; Zhao, Y.; Wang, J. Cellulose Dissolution at Ambient Temperature: Role of Preferential Solvation of Cations of Ionic Liquids by a Cosolvent. *Carbohydr. Polym.* **2013**, *92*, 540–544.
- (15) Liu, H.; Sale, K.; Holmes, B.; Simmons, B.; Singh, S. Understanding the Interactions of Cellulose with Ionic Liquids: A Molecular Dynamics Study. *J. Phys. Chem. B* **2010**, *114*, 4293–4301.
- (16) Gross, A. S.; Bell, A. T.; Chu, J. Thermodynamics of Cellulose Solvation in Water and the Ionic Liquid 1-Butyl-3-Methylimidazolium Chloride. *J. Phys. Chem. B* **2011**, *115*, 13433–13440.
- (17) Payal, R.; Bharath, R.; Periyasamy, G.; Balasubramanian, S. Density Functional Theory Investigations on the Structure and

Dissolution Mechanisms for Cellobiose and Xylan in an Ionic Liquid: Gas Phase and Cluster Calculations. *J. Phys. Chem. B* **2012**, *116*, 833–840.

(18) Kirschner, K. N.; Yongye, A. B.; Tschampel, S. M.; Gonzalez-Outeirino, J.; Daniels, C. R.; Foley, B. L.; Woods, R. J. GLYCAM06: A Generalizable Biomolecular Force Field. *Carbohydrates. J. Comput. Chem.* **2008**, *29*, 622–655.

(19) Wu, Y. J.; Tepper, H. L.; Voth, G. A. Flexible Simple Point-Charge Water Model with Improved Liquid-State Properties. *J. Chem. Phys.* **2006**, *124*, 024503.

(20) Cornell, W. D.; Cieplak, P.; Bayly, C. I.; Gould, I. R.; Merz, K. M.; Ferguson, D. M.; Spellmeyer, D. C.; Fox, T.; Caldwell, J. W.; Kollman, P. A. A Second Generation Force Field for the Simulation of Proteins, Nucleic Acids, and Organic Molecules. *J. Am. Chem. Soc.* **1995**, *117*, 5179–5197.

(21) Yang, L.; Huang, K.; Yang, X. Dielectric Properties of *N,N*-Dimethylformamide Aqueous Solutions in External Electromagnetic Fields by Molecular Dynamics Simulation. *J. Phys. Chem. A* **2010**, *114*, 1185–1190.

(22) Liu, Z. P.; Huang, S. P.; Wang, W. C. A Refined Force Field for Molecular Simulation of Imidazolium-based Ionic Liquids. *J. Phys. Chem. B* **2004**, *108*, 12978–12989.

(23) Frisch, M. J.; Trucks, G. W.; Schlegel, H. B.; Scuseria, G. E.; Robb, M. A.; Cheeseman, J. R.; Scalmani, G.; Barone, V.; Mennucci, B.; Petersson, G. A.; et al. *Gaussian 09*, version B.01; Gaussian, Inc.: Wallingford, CT, 2009.

(24) Liu, X.; Zhang, S.; Zhou, G.; Wu, G.; Yuan, X.; Yao, X. New Force Field for Molecular Simulation of Guanidinium-Based Ionic Liquids. *J. Phys. Chem. B* **2006**, *110*, 12062–12071.

(25) Lyubartsev, A. P.; Laaksonen, A. M.DynaMix—A Scalable Portable Parallel MD Simulation Package for Arbitrary Molecular Mixtures. *Comput. Phys. Commun.* **2000**, *128*, 565–589.

(26) Tuckerman, M.; Berne, B. J.; Martyna, G. J. Reversible Multiple Time Scale Molecular-Dynamics. *J. Chem. Phys.* **1992**, *97*, 1990–2001.

(27) Deleeuw, S. W.; Perram, J. W.; Smith, E. R. Simulation of Electrostatic Systems in Periodic Boundary-Conditions. 3. Furture Theory and Applications. *Proc. R. Soc. London, Ser. A* **1983**, *388*, 177–193.

(28) Martinez, L.; Andrade, R.; Birgin, E. G.; Martinez, J. M. PACKMOL: A Package for Building Initial Configurations for Molecular Dynamics Simulations. *J. Comput. Chem.* **2009**, *30*, 2157–2164.

(29) Martyna, G. J.; Tuckerman, M. E.; Tobias, D. J.; Klein, M. L. Explicit Reversible Integrators for Extended Systems Dynamics. *Mol. Phys.* **1996**, *87*, 1117–1157.

(30) Tokuda, H.; Hayamizu, K.; Ishii, K.; Susan, Md. A. B. H.; Watanabe, M. Physicochemical Properties and Structures of Room Temperature Ionic Liquids. 1. Variation of Anionic Species. *J. Phys. Chem. B* **2004**, *108*, 16593–16600.